

Accepted Manuscript

Title: Architecture for the efficient manufacturing by printing of heated, planar, resistive transducers on polymeric foil for gas sensing

Authors: José Luis Ramírez, Fatima E. Annanouch, Eduard Llobet, Danick Briand



PII: S0925-4005(17)32239-6
DOI: <https://doi.org/10.1016/j.snb.2017.11.108>
Reference: SNB 23602

To appear in: *Sensors and Actuators B*

Received date: 12-8-2017
Revised date: 27-10-2017
Accepted date: 20-11-2017

Please cite this article as: José Luis Ramírez, Fatima E. Annanouch, Eduard Llobet, Danick Briand, Architecture for the efficient manufacturing by printing of heated, planar, resistive transducers on polymeric foil for gas sensing, *Sensors and Actuators B: Chemical* <https://doi.org/10.1016/j.snb.2017.11.108>

This is a PDF file of an unedited manuscript that has been accepted for publication. As a service to our customers we are providing this early version of the manuscript. The manuscript will undergo copyediting, typesetting, and review of the resulting proof before it is published in its final form. Please note that during the production process errors may be discovered which could affect the content, and all legal disclaimers that apply to the journal pertain.

Architecture for the efficient manufacturing by printing of heated, planar, resistive transducers on polymeric foil for gas sensing

José Luis Ramírez^{a,1,*}, Fatima E. Annanouch^{b,2}, Eduard Llobet^b, Danick Briand^a

^a Ecole Polytechnique Fédérale de Lausanne, Institute of Microengineering, MC B4 (Microcity), Rue de la Maladière 71b, CP 526. Switzerland.

^b Universitat Rovira i Virgili, Departament d'Enginyeria Eléctrica, Electrónica i Automàtica, ETSE, Av. Països Catalans 26, 43007 Tarragona. Spain.

¹ Permanent address: Universitat Rovira i Virgili, Departament d'Enginyeria Eléctrica, Electrónica i Automàtica, ETSE, Av. Països Catalans 26, 43007 Tarragona. Spain.

² Permanent address: IM2NP, IMT-Technopôle de Château Gombert, 38, rue Joliot-Curie, 13451 Marseille Cedex 20, France.

e-mail addresses:

joseluis.ramirez@urv.cat , fatima.annanouch@im2np.fr , eduard.llobet@urv.cat , danick.briand@epfl.ch

* Corresponding author: joseluis.ramirez@urv.cat (J. L. Ramírez)

Highlights

- A new architecture has been proposed for planar heated resistive gas sensors.
- It uses one of the sensing electrodes simultaneously as heating element.
- It consumes less metallic ink and substrate area than a usual planar configuration.
- Thus, it enhances power consumption and thermal homogeneity.
- It avoids printing robust interdielectric layer as in stack configurations.

Abstract

This paper presents a new coplanar architecture to implement the electrodes and the heating element of printed gas sensors. The design includes two electrodes and three contacts. One of the electrodes works as heating element and, simultaneously, drains the sensing current. The electrical modelling of the transducers and its electronic implementation are reported. As this new approach is related to the electrical topology of the system, a reduction in the number of conductive elements will be obtained for any geometry, deposition method, and gas sensing layer. Compared with other coplanar topologies, this approach simplifies the transducers processing to a single printing step, avoiding the use of an interdielectric layer between heater and electrodes, and reducing the amount of electrically conductive ink necessary to pattern heater and electrodes of the transducers. This cost-effective architecture and process was applied to the fabrication of heated transducers for metal-oxide gas sensors. The two electrodes were made by inkjet printing of gold on polyimide foil. For the validation of the concept, a Pt loaded WO₃ sensing layer was grown on top of these transducers printed with the proposed topology. When tested against H₂, diluted in air, their response was as good as the one obtained employing the classical topology. This simple architecture has strong potential for the realization of fully printed resistive gas sensors and can be implemented as well in clean room processed transducers.

Keywords: printing, planar transducer, heating, resistive gas sensor.

1. Introduction

Chemo-resistive gas sensors based on metal oxide sensing layers have attracted much interest in the past years, as a low cost approach for gas sensing [1]. The usual read-out architecture relies in measuring the active layer variable resistance using a pair of electrodes. Their commercial version operates at relatively high temperatures for optimum performances in term of sensitivity and selectivity [2], which has required the implementation of a joule heating element. This heating element can be integrated in the same plane as the sensing electrodes, having a co-planar architecture, or more often, in a different one, below the electrodes, resulting in a stacked topology.

When implementing the heater in a stacked approach with the electrodes, two possible approaches have been considered for the insulating dielectric layer between the heater and the electrodes. In one, the substrate itself is used with the electrodes placed on one side, while the heater is placed in the reverse side [3]. This approach has been used for many years in screen printed transducers made on alumina substrates with platinum used as heater and electrodes. Recently, this approach has been applied to fabrication of heated transducers on a 50 μm -thick polyimide foil for a fully printed metal-oxide gas sensor [4]. This configuration results in relatively high power consumption since heat has to flow across the thickness of the substrate to reach warm up sensing layer on the other side. In the other, the heater and the electrodes are stacked on the same side of the substrate with a thin dielectric insulator resulting in reduced power consumption [5], which is the architecture mainly used in silicon micromachined hotplate type metal-oxide gas sensors. The implementation of this approach for the realization of fully printed gas sensors, by inkjet for instance, is a real challenge. It requires the development of a polymeric dielectric layer withstanding the high temperature needed for the annealing of the metal-oxide film itself and for the operation of the sensor. Moreover, inks solvent orthogonality is necessary for printing heater, dielectric, electrodes and sensing layers, and topography issues must be faced when printing multi-layers. Finally, using an inter-dielectric involves the proper printing of the electrodes on this layer with good resolution and adhesion. In both cases, using the substrate or a thin dielectric layer to insulate the heater from the electrodes, two or more patterning steps are needed to fabricate heater and electrodes.

When the transducers architecture is reduced to one layer, mainly to cut production cost, the usual solution is a perimeter heater close and coplanar to two electrodes [6] [7]. But including heater and electrodes on the same plane represents an increase of the area of the transducer and therefore an increase in the power needed to rise the sensor temperature. Polymers that can be considered as substrate for printed metal-oxide gas sensors, i.e. polyimides, are poor heat-conductors and are interesting to minimize power consumption. However, because of their low thermal conductivity, a planar configuration of the transducer, in which the heater surrounds the electrodes, is not optimum for achieving a good thermal distribution over the sensing area.

We have found only one publication [8] that uses the heating electrode as draining node when sensing. However, far from draining while simultaneously heating, the full circuit is used in a time sharing mode: part time heating, part time measuring, therefore, no continuous operation is possible. This forces a switched working mode in which, while the heater is fully grounded, the measurement time should be short enough to finish before the device has cooled below the proper working temperature. This represents a serious limitation for some active layers. Or, if a transient analysis approach is adopted, only data when cooling down can be collected as no measurement can be taken when switching on the heating power. Moreover, the implemented circuit is classically designed with two sensing electrodes, one heating track and four contacts (plus two for the heater resistance measurements), so there is no improvement envisioned in the fabrication process.

Here, we are reporting on a co-planar topology that is notably of high interest for the simple manufacturing of metal-oxide gas sensors by printing. We propose to use one of the sensing electrodes, simultaneously, as the heating track. We explain how, by wisely biasing one of the sensing electrodes, the heater track can deliver steady power while simultaneously serving as drain electrode for the sensing

current. This design includes two electrodes and three contacts only, which results in a reduced number of conductive elements, decreases substrate area needed in a planar configuration and simplifies transducer processing to a single printing step. It avoids printing an inter-dielectric layer between heater and electrodes, and reduces the amount of expensive metallic ink necessary to pattern heater and electrodes. This results in a cost-effective architecture and process for producing simple transducers for resistive gas sensors that, similarly to conventional transducers, are still able to operate in continuous heating mode (or whatever switched mode is chosen with no time or phase restriction). Proper operation of the printed flexible transducer has been proven and its implementation for gas sensing demonstrated with results comparable with classical silicon based transducers.

2. New architecture

2.1 Topology of the architecture

The classical topologies for heated resistive sensors require at least three electrically conductive elements: two sensing electrodes plus a heater, with usually two contacts each for reading and biasing them, respectively. We propose the use of just two conductive electrodes with three contacts only. One of the sensing electrodes acts as well as the heating element. Two of the contacts are located at both ends of the electrode acting as sensing and heating element and the third one is linked to the second sensing electrode. The ground contact of the heating electrode will drain both the heating and the sensing currents. In Figure 1 a schematic representation of the proposed topology is shown: just one pair of electrically conductive electrodes, one active sensing layer connected by both electrodes with only three electrical contacts.

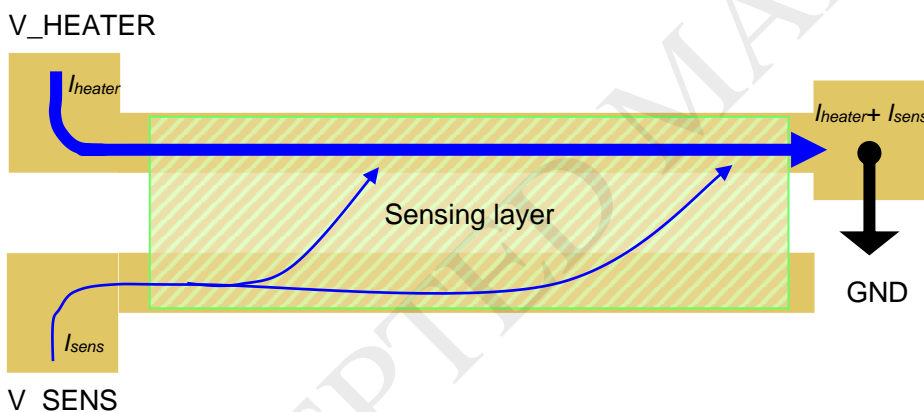


Figure 1 Schematic representation of the proposed topology: two electrodes and three contacts.

To measure the variation of resistance of the sensor in the applicative environment, any viable electronics ends the read-out chain feeding a voltage to the Analog to Digital Converter (ADC) input of a microcontroller. Therefore, the sensor should be either biased with a known current in order to measure the voltage between its terminals or biased with a known voltage to measure the current flowing through it. The latter can be converted to an ADC readable voltage by means of a transconductance amplifier.

Having in mind the use of an integrated potentiostat, in a future microcontroller-based system, we have chosen to bias the sensor with a known voltage and therefore to measure the sensing current. It results that only one terminal (one external contact, V_{SENS} in figure 1) is needed to polarize one end of the active sensing layer and to measure the current injected through it (I_{sens}). Once this current has gone through the sensing layer, it can be drained by the reference node of the transducer (GND) with no additional contact

needed. Moreover, there is no need to print an additional electrode to connect the sensing layer to GND. It can be reached through the heater electrode, despite it is not fully grounded.

2.2. Parameter model

In this work, we have been developing this transducer architecture for metal-oxide gas sensitive layers. Typically, the metal oxide sensors operate at high temperature (150 to 400°C). The best materials for the electrodes are noble metals such as platinum and gold. These metallic electrodes, in comparison to the metal-oxide film and the plastic foil, become the main contributor to the overall cost of the sensor fabrication. Based on electrical conductivity of the materials involved, we have analyzed a distributed parameter model for the circuit, which is shown in Figure 2.

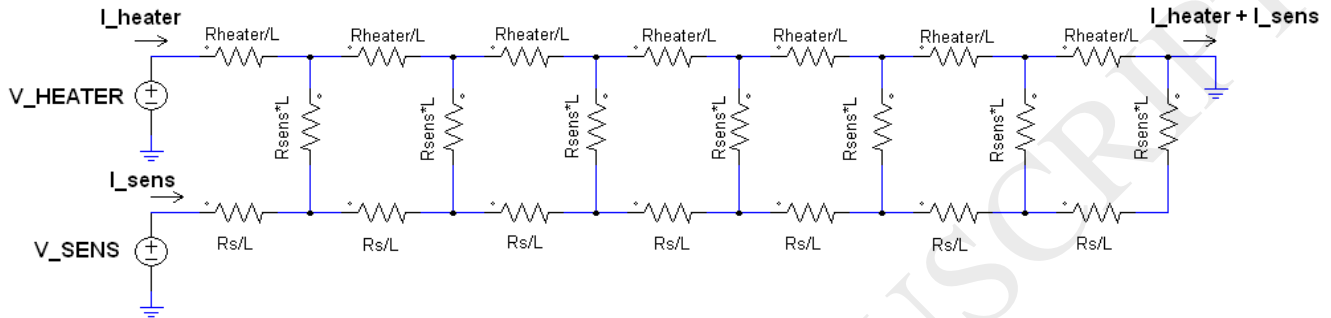


Figure 2 Distributed parameter model of the proposed topology.

Being the active sensing layer an *n*-type or *p*-type material (e.g., a metal oxide nanomaterial) and the electrodes metallic (e.g. gold or platinum), the resistance of the gas-sensitive film will typically be several orders of magnitude higher than the one of the electrodes (e.g. $R_{metal-oxide} \gg R_{Au}$). Choosing by design specification the sensing electrode bias voltage to be higher than the heater bias voltage ($V_{sens} > V_{heater}$) ensures that the current through the gas sensitive layer is always flowing from the sensing electrode to the heater electrode. In addition, since the heater current is large compared to the added sensing current, it can be assumed that there will not be significant changes in the bias point of the heating element, despite that changes occur in R_{sens} during gas detection events. For the case described (i.e., $R_{heater} \approx R_s \ll \ll R_{sens}$), the concentrated parameter model shown in Figure 3 is a very good approximation to what is described in Figure 2.

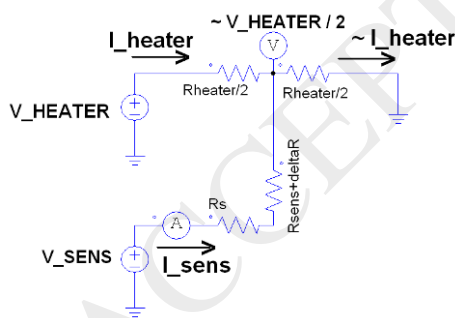


Figure 3 Concentrated parameter model of the proposed topology.

In our case, the resistance of the active layer used (i.e. Pt-WO₃) is near five orders of magnitude higher than the heater metallic resistance ($R_{sens} \approx 10^5 \times R_{heater}$), so the heater bias can be assumed to be constant, even in the case of a gas detection event that may cause a decrease in the resistance of the active film, resulting in a negligible error. Therefore, the measured injected sensing current (I_{sens}) allows to compute the resistance of the active layer according to Eq. (1).

$$R_{sens} = (V_{sens} - V_{heater}/2) / I_{sens} \quad (1)$$

Where V_{sens} , as shown in Figure 4, is set by the user and driven by the same transconductance amplifier, which delivers as output a voltage proportional to I_{sens} , as shown in Eq. (2).

$$V_{out} = V_{sens} + I_{sens} \times R_{TIA} \quad (2)$$

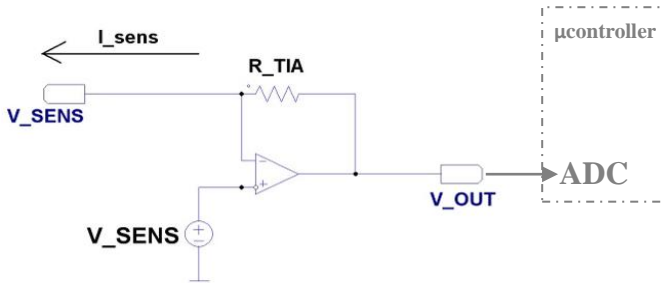


Figure 4 Transconductance amplifier: It forces a bias V_{sen} and outputs a voltage proportional to the injected current.

When read by an ADC, V_{out} allows a microcontroller to compute R_{sens} according to Eq. (3)

$$R_{sens} = R_{TIA} \times (V_{sens} - V_{heater}/2) / (V_{OUT} - V_{sens}) \quad (3)$$

Even for an R_{sens} just an order of magnitude bigger than R_{heater} , which would imply a very unlikely 4-order of magnitude drop in the resistance of the sensing layer during a detection event, this still represents a good approximation. It is easy to determine, by the superposition theorem, that the sensing current drain node voltage, which has been approximated as $V_{heater}/2$ in Eq. 3, is more precisely $0.48 \cdot V_{heater} + 0.04 \cdot V_{sens}$. This difference is small and it can be easily compensated via the software of the microcontroller, so we can rely on the simplified model to understand the behaviour of the architecture.

3. Results

3.1. Processing of the transducers via printing and their electro-thermal simulation and characterization

In order to demonstrate the viability of the approach and to develop FEM models for improving their thermal design a series of transducers were fabricated, following the proposed architecture and with a geometry well suited for their thermal characterization, as illustrated in Figure 5. A 50 μm - thick film of Kapton 200EN, a polyimide from Dupont®, was used as substrate. After treating the surface with a mild oxygen plasma to make it more hydrophilic (which result in printing of single dots bigger than 200 μm diameter), the electrode pattern was ink jet printed with a Dimatix Materials Printer (DMP-2800).

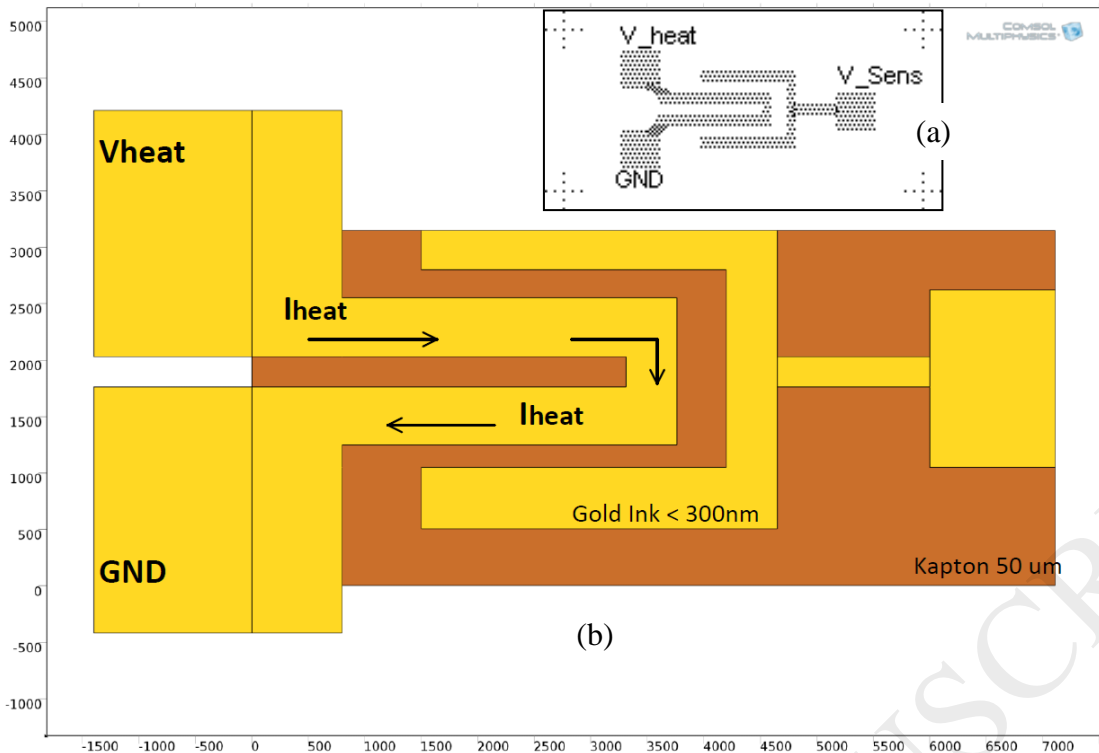


Figure 5 Device layout: (a) First layer bmp pattern feed to materials printer. (b) Schematic geometry used for the Comsol simulation (X-Y coordinates in μm).

Platinum ink not being available at the time of this work, the ink used from Harima Chemical Group (NPS series) was made of gold nanoparticles in solution. In order to obtain a satisfactory sheet resistance and to ensure electrical continuity, a stack of 4 layers was printed. Taking advantage of the different behaviour of the ink drops when in contact with Kapton and with already printed gold layers, we choose to build a pyramidal profile for these metallic tracks. The topology of the first layer was dominated by the coffee ring effect limited by side by side drop contact, resulting in a honeycomb structure with not a full coverage of the substrate by the gold ink. The second layer behaved the same but the honeycomb patterned was shifted and full coverage of the substrate was obtained. The third layer printed over gold only exhibited quite uniform drops on top of the previous structure. The fourth layer ended in compact drops with a dome shape. After annealing the ink for 90 min in an oven at 250°C , a set of transducers were obtained that exhibited a heater resistance of about $30\ \Omega$ (Figure 6). The resulting track width was $350\ \mu\text{m}$, and the inter-electrode gap $250\ \mu\text{m}$.

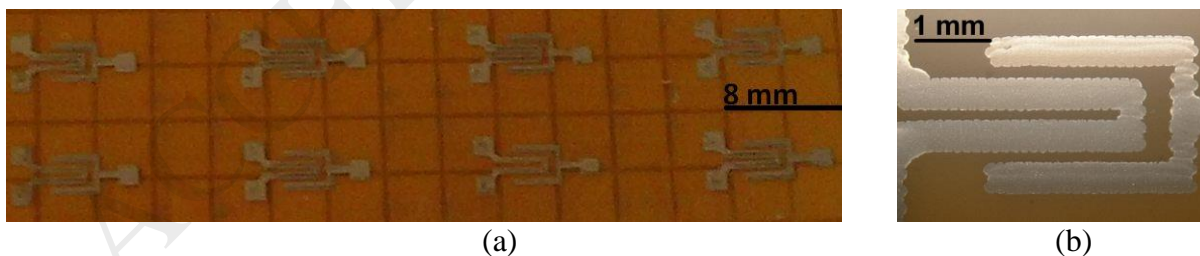


Figure 6 (a) The set of transducers with two gold electrodes and 3 contacts, inkjet printed on Kapton. (b) Device close up.

The average picture of the printed gold lines, by construction, looked like a ziggurat over a honeycomb basis, but in a close up, the thickness is quite random. The profile and thickness of the metallic lines were analyzed using a white light interferometer (Wyko NT 110 from Veeco) and a KH 8700 Hirox 3D digital microscope, but the gold layer was too thin and non-homogeneous, and the flexible substrate too uneven, to get a reliable measurement. Analysis of the collected data resulted in a variable thickness from $20\ \text{nm}$ to $300\ \text{nm}$ with a very heterogeneous distribution. This was due partly to the randomness in the impact of the drops when jetted over the slightly irregular substrate, and mainly to the geometry of the stacked

layers and the coffee ring effect experienced. Figure 7 shows the optical image of a device when illuminated from its backside, four stacked layers can be differentiated: the bottom one highly spread and nearly transparent, the two in the middle with clear coffee ring effect and the top one much darker since it is compact and thick.

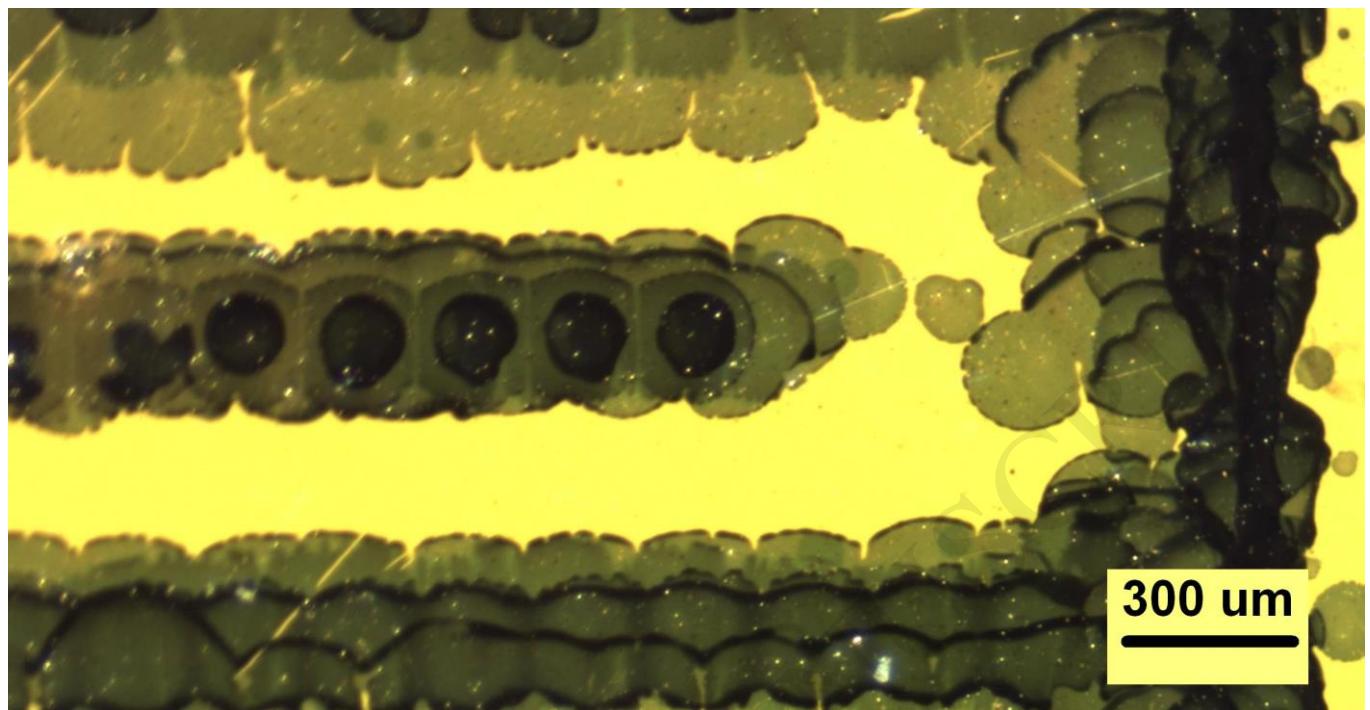


Figure 7 Back lighted view of tracks printed in four pyramidal stacked layers.

The transducer was electro-thermally characterized by an external independent institute (FEMTO-ST, Besançon - France) using micro-thermocouple (S type, 1.3 μm in diameter [9]) to measure the surface temperature of the device. Experimental characterization of the temperature distribution was carried out by measuring the temperature in 16 different points, while applying a bias current through the heater. Setting a polarization heater current $I_{heater} = 70 \text{ mA}$ resulted in a temperature at the center of the device of $T_{cent} = 208 \text{ }^\circ\text{C}$, with a power consumption of 158 mW. Temperature was measured at points shown in Figure 8.

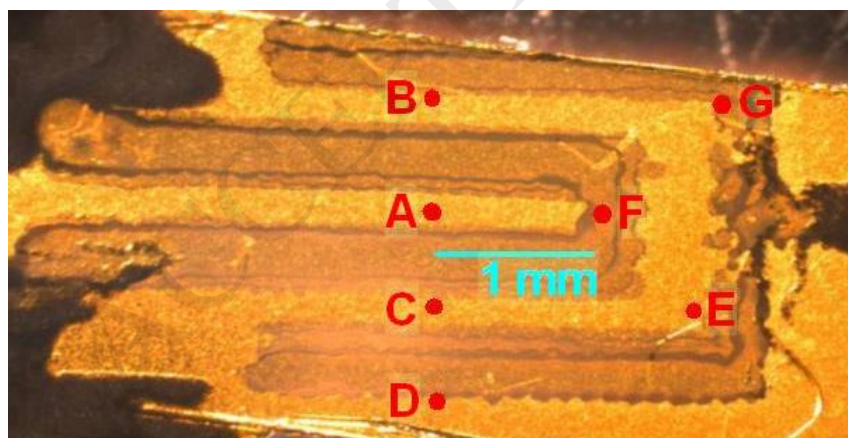


Figure 8 Placement of points where surface temperature was experimentally measured.

In parallel to the physical characterization, we proceeded to a FEM simulation with Comsol Multiphysics using the basic DC current module coupled with the thermal module through the Joule effect. That “coupling” means that the thermal module takes into account heat generated by power dissipation in resistors, and the DC current module takes into account the temperature reached to determine the resistance values applying a linear variation $\rho = \rho_0 \cdot (1 + \alpha \cdot (T - T_0))$. The temperature coefficient of

resistance of the printed-gold was obtained measuring the electrodes resistance while placed inside an oven with a slow increasing temperature ramp. For the temperature range of interest (from T_{amb} to 300 °C), a temperature coefficient $\alpha = 0.00165 \text{ K}^{-1}$ was obtained (i.e., half the coefficient of pure gold $\alpha_{Au} = 0.0034 \text{ K}^{-1}$). The electrical resistivity of the gold material was taken from data sheet and a constant thickness was set that would fit the measured total resistance value of the device. That did not give the exact result at every point, but has shown to be very accurate in average.

Once the device geometry is defined, to run the electro-thermal simulations boundary conditions need to be applied. As electrical boundary conditions we defined all around (3D) insulation, but the perimeter of the bonding pads were set to the bias voltage (*Vheat* and *GND*, respectively) through a contact resistivity of $\rho_{contact} = 2.58 \times 10^{-9} \text{ } \Omega\text{m}^2$ (which resulted in a 2 Ω serial resistor at the input of each contact). That does not exactly match reality, as the full pad is supposed to be at bias voltage, but it is a very good approximation, being the easiest way to include the contact resistance and represented a more realistic behaviour of the electrical current flow through the pad. The sensing contact was set as isolated at this stage of characterization.

As thermal boundary conditions we used the model provided by Comsol. Despite a 2D simulation was run (to save time and computational resources) an “out of plane” option was activated. Then, to reproduce the experimental characterization where the device was lying flat on the measurement equipment, we set “natural perpendicular upwards convection” for the front side of the device, “natural perpendicular downwards convection” for its back side, and “natural parallel convection” for the 50 μm -thick perimeter. Finally, we set the bonding pads as constant T_{amb} since, once the wires bonded, they will act as nearly-perfect heat drains. All material parameters, boundary conditions and simulation set ups have been included in supporting information (Supporting information: 3. Simulation parameters pp. 2-4).

The temperature surface distribution obtained from the simulation is shown in Figure 9.

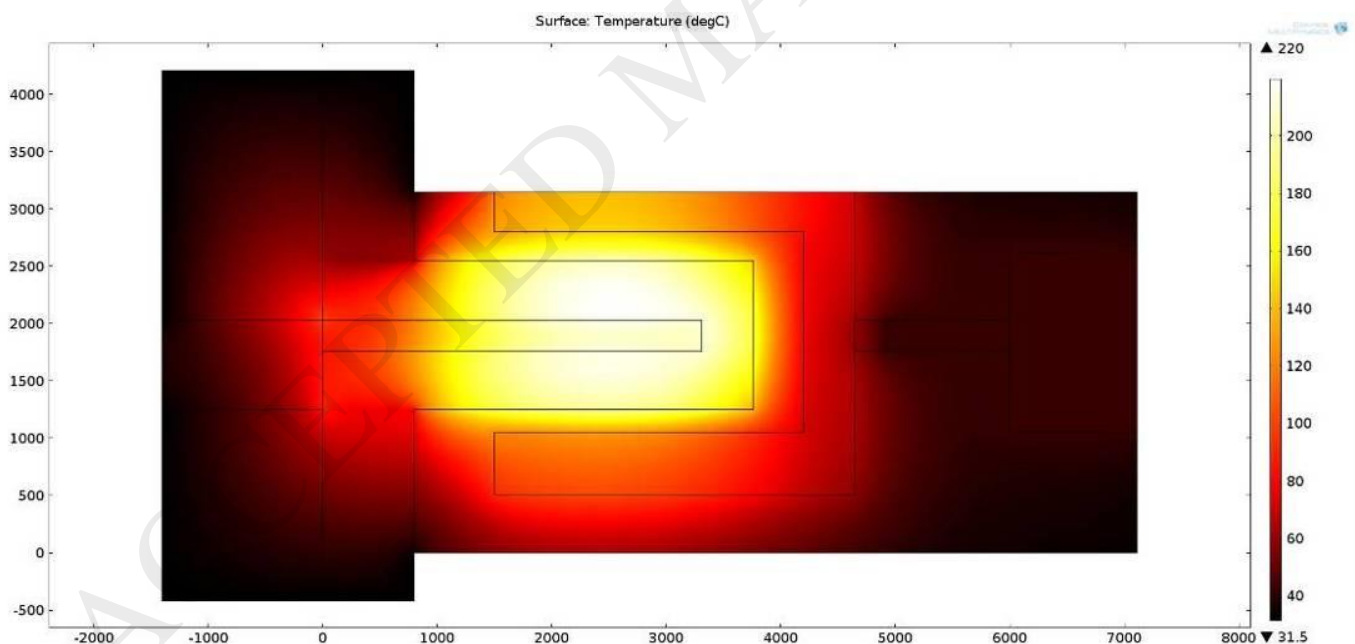


Figure 9 Temperature surface distribution as simulated by Comsol (X-Y coordinates are in μm).

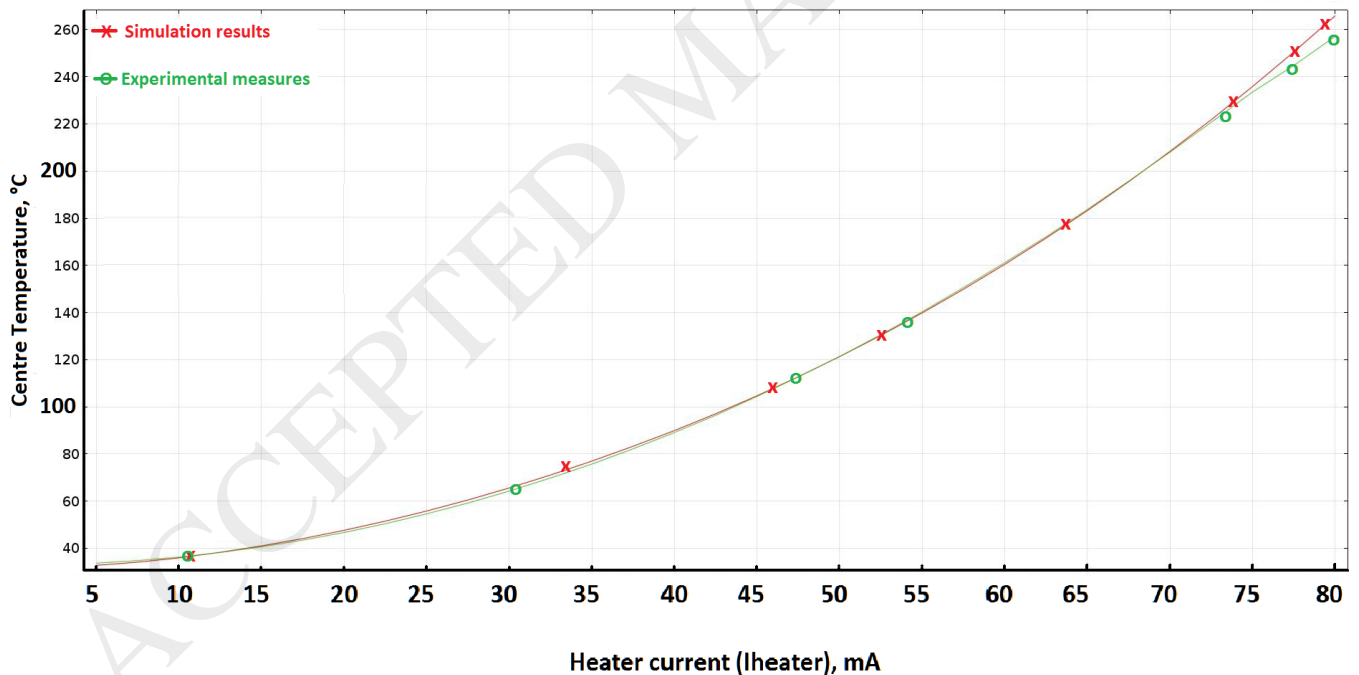
Simulation results fitted extremely well the experimental measurements. To better appreciate how close the figures are, for every measurement point Table 1 shows: the simulated temperature, the absolute temperature difference between simulation and experimental measurements, and the difference relative to the expected temperature increase over $T_{amb}=31 \text{ } ^\circ\text{C}$ (%).

Table 1 Simulated temperatures, difference to measured ones and relative error in expected heating.

Point	T_{sim} (°C)	$T_{measur} - T_{sim}$ (°C)	$ T_{measur} - T_{sim} / T_{sim} - T_{amb} $ (%)
A	209.21	-0.92	0.5
B	159.05	-5.07	4.0
C	155.92	-11.88	9.6
D	106.28	-1.57	2.1
E	96.05	2.95	4.6
F	200.50	1.50	0.9
G	77.94	3.37	7.3

In the sensing area, far away from the bonding pads, the deviation is lower than 10% (Table 1). Measurements and simulations were performed to know the temperature at the center of the device for different heater polarization currents. The results are shown in Figure 10. As can it be seen, there is a nearly perfect match below 220 °C (i.e., for less than 72 mA heating current), and the difference is even lower than 5% above 250 °C.

Let us point out that we found useful to include, in our simulations, heat losses due to out of plane radiation. In spite of the fact that radiation losses are generally considered to be negligible below 400 °C for devices with smaller active areas [9][11][12], our results start to diverge at around 60 °C and reach a 10% error at a temperature as low as 250 °C. The consideration of radiation prevents introducing errors on the temperature values higher than 20 °C, which would be significant for the design of metal oxide gas sensors. So we set emissivity for the polyimide and gold at $E_{PI}=0.7$ and $E_{Au}=0.12$, respectively. Emissivity figures were initially taken from tables [13] and later on fine-tuned to fit the results, as they depend on final roughness and the thermal post-treatment of the surface of the sintered gold layer.

**Figure 10** Temperature at the centre of the device vs. heater current, measured and simulated, at $T_{amb} = 31$ °C.

These results completely validate the simulation model. Therefore, the surface distribution and behaviour of currents, voltages and temperatures of our proposed topology is confirmed. Moreover, it can be employed as a valuable tool for designing new devices with different three-dimensional geometries (i.e. different 2D patterns and/or different substrate and printed tracks thickness).

3.2. Gas sensors results

Pt-nanoparticle decorated WO_3 nanowires were directly grown on top of the electrodes printed over the polyimide substrate by means of aerosol assisted chemical vapour deposition (AA-CVD) using a hot wall reactor. A summary of the process used is as follows. Tungsten hexacarbonyl and hydrogen hexachloroplatinate were mixed and dissolved in a 50:50 mixture of acetone and methanol. An aerosol generator was employed to produce sub-micrometer-sized aerosol droplets, which were transported by a nitrogen flow to the heated reaction zone in which the substrate to be coated was held. Reaction temperature was set to 380°C and the deposition process took 10 min to complete. To prevent the contacts to be covered by the metal oxide layer, which would result in an increased contact resistance, a shadow mask was used (of the same flexible Kapton material) to protect the contact areas. More details on the growth process can be found elsewhere [14].

The AA-CVD process implemented resulted in the growth of randomly oriented tungsten oxide nanowires completely covering the exposed electrode area of the sensor chip. Figure 11 illustrates these results. Typically, nanowires were 60 to 120 nm in diameter and about 7 microns in length. The nanowires were homogeneously decorated with a mono-modal distribution of Pt nanoparticles having an average diameter of 2.5 nm. Tungsten oxide nanowires were single crystalline, monoclinic phase and slightly sub-stoichiometric. XPS results indicate that the outer shell of nanoparticles consists of PtO, and that metal loading is about 3% at [15].

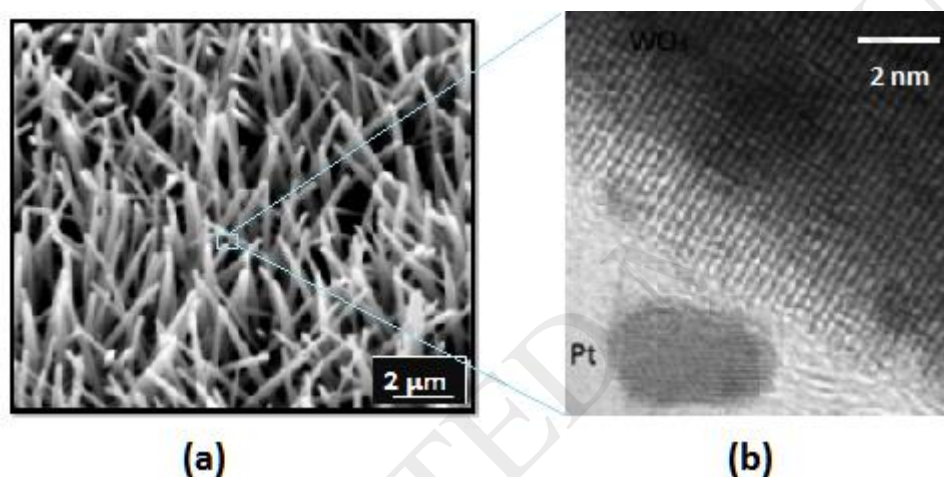


Figure 11 (a) SEM micrograph showing the morphology of the tungsten oxide nanowire film on top of the electrode area. (b) Close-up, HR-TEM micrograph showing a Pt nanoparticle on the surface of a tungsten oxide nanowire.

At this point we could prove our initial statement: the variations of resistance of the active layer could be measured while one of the electrodes was working as a heater. Different sensing polarization voltages (V_{sens}) at different heater polarization voltages (V_{heater}) were applied and the corresponding current through the sensing electrode (I_{sens}) was measured. Figure 12 shows the results, where the horizontal axis corresponds to the voltage drop in the active layer $V_{sens_eff} = V_{sens} - V_{heater}/2$ (mV), and the vertical axis corresponds to the sensing current I_{sens} (μA).

Sensing current vs. biasing voltage, at different heater temperatures

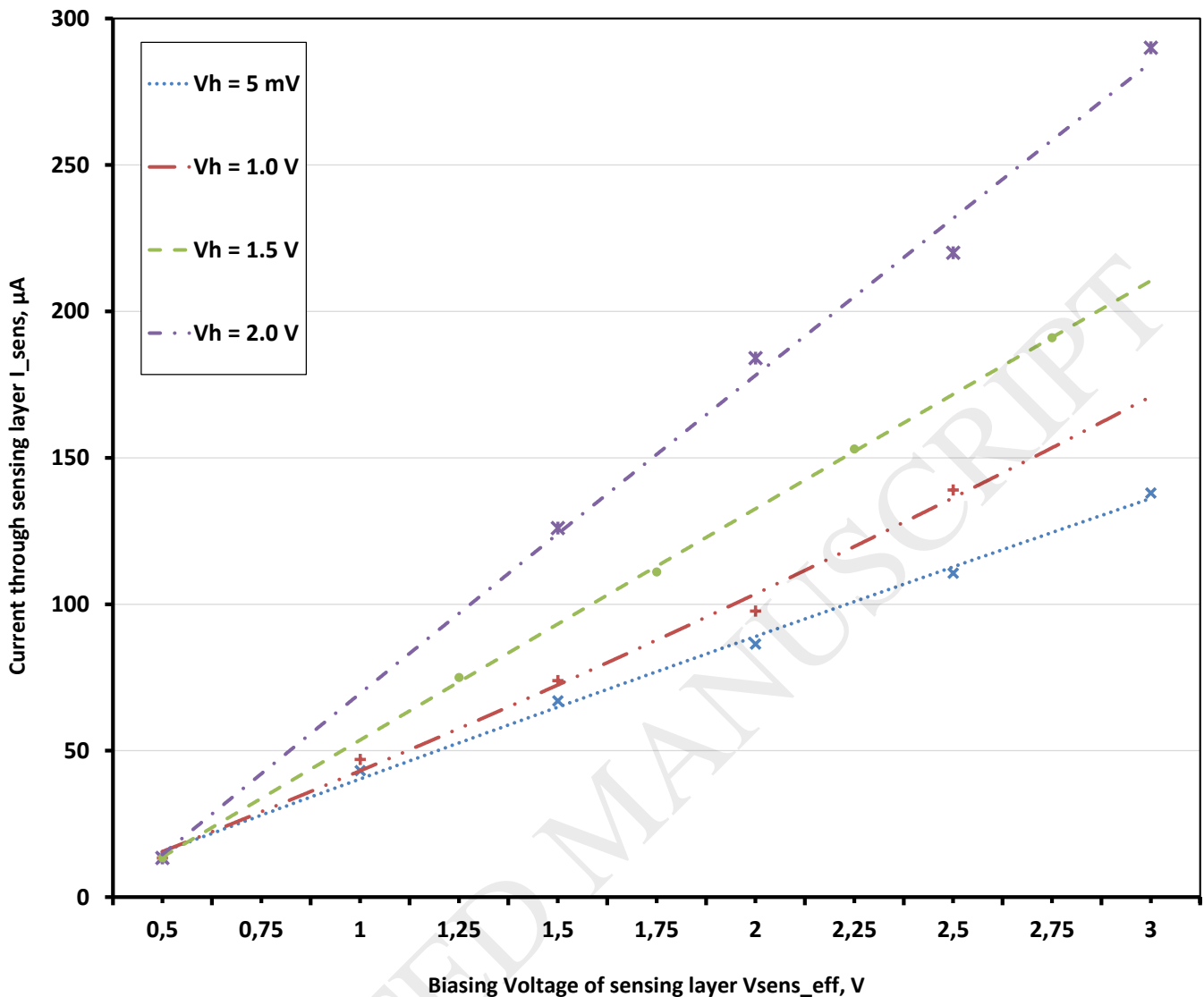


Figure 12 I_{sens} (μA) vs. V_{sens_eff} (mV) at different heater polarizations (V_h).

The results obtained were as expected. For a chosen heater polarization, the current through the active layer increased linearly as the applied voltage increased. And for increasing heater voltage polarization, so when the device temperature rose, the active layer resistance went down (i.e. $\Delta I_{sens}/\Delta V_{sens_eff}$ grew). This behaviour matches the one of traditional hotplates architectures, as can be seen in the supporting information (Supporting information: 1. Classical device behaviour pp. 1).

Once the devices were characterized and the feasibility demonstrated, we produced a new set of electrodes specifically intended to be used for gas sensing measurements. Exactly the same two steps fabrication process was used: Harima gold nanoparticles ink was inkjet printed to form the electrodes over a Kapton foil and the Pt-WO₃ nano-wires directly grown by AA-CVD to obtain the active layer. The layout and the ink jet printed set can be seen in Figure 13(a,b). The same architecture was used, but with a slight variation in geometry: this time the transducer used was the usual pair of interdigitated electrodes seen for this type of gas sensors. It has to be pointed out that, as it can be seen in Figure 13(a), five contacts were printed instead of the three proposed. The two in excess were just for testing purposes. As it can be clearly seen, one was short-circuited to the heater contact (V_h) and the other one to ground contact (gnd). They were intended to facilitate a four wire measurement of the heater resistance, so the contact resistance could be easily identified (a constant to be subtracted when computing the temperature value

from the resistance variations, as seen in the section on “*Simulations results*”). This was necessary only for testing the prototype, in production the initially proposed three contacts topology would be used. Device were bonded to a PCB, wire suspended, to facilitate its electrical connection to the measurement set up while ensuring its thermal isolation as shown in Figure 13(c).

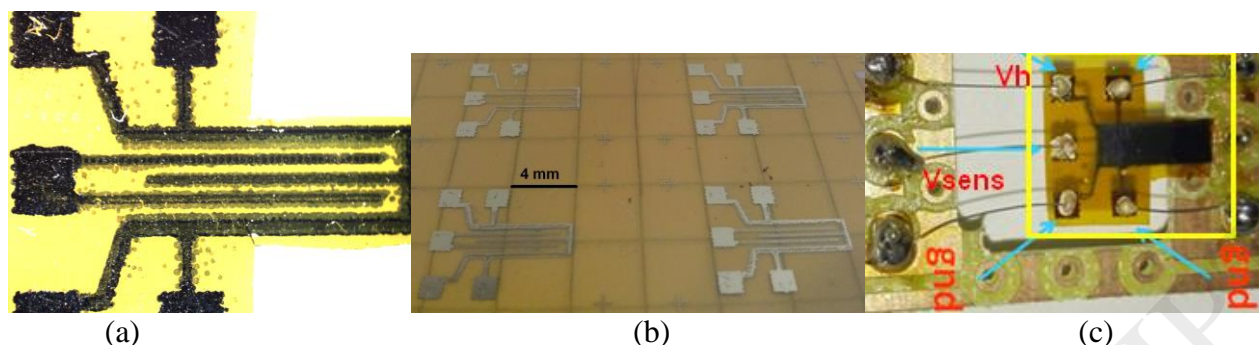


Figure 13 Tested devices: (a) Back-lighted image close-up, (b) Inkjet printed series, (c) Pt-WO₃ covered sample.

In order to compare their performance with a silicon micro-machined buried-heater WO₃ sensor fabricated using AA-CVD [16], devices were tested against H₂, at heater power consumption of 14.87 mW/mm², with very good results. Tests were carried out in a Teflon and stainless steel chamber, the volume of which was 20 cm³. Through the inlet it was injected a continuous flow of 200 sccm. The carrier was synthetic air at 10% RH. The desired concentrations of H₂ were obtained through the use of calibrated gas bottles and two computer driven mass flow controllers from Bronkhorst High-Tech B.V. (NL). In case any other target gas should be tested, as shown in the selectivity study provided in the supported information, it results quick and easy just to change the calibrated bottle to one of that new gas target. This system is even fitted to measure gas mixtures by simply connecting a second calibrated bottle to the third mass flow controller which is included.

Figure 14.a shows the response curve to different hydrogen concentrations. Response was defined as the ratio I_g/I_o , where I_o is the current flowing through the gas sensitive film when exposed to reference air, while I_g is the current when the sensor is exposed to a given concentration of hydrogen diluted in air. Figure 14.b shows the dynamic response of the current for successive response and recovery cycles of increasing hydrogen concentrations. While Figure 14.a shows that a remarkable sensitivity to hydrogen was obtained, Figure 14.b demonstrates the reversibility of the detection and good baseline stability of the sensors. These results compare well with the performance obtained with equivalent gas sensing materials grown on MEMS silicon transducers. Further details on sensor selectivity and temperature dependence can be found in supporting information (Supporting information: 2. Sensor response to different conditions pp 2).

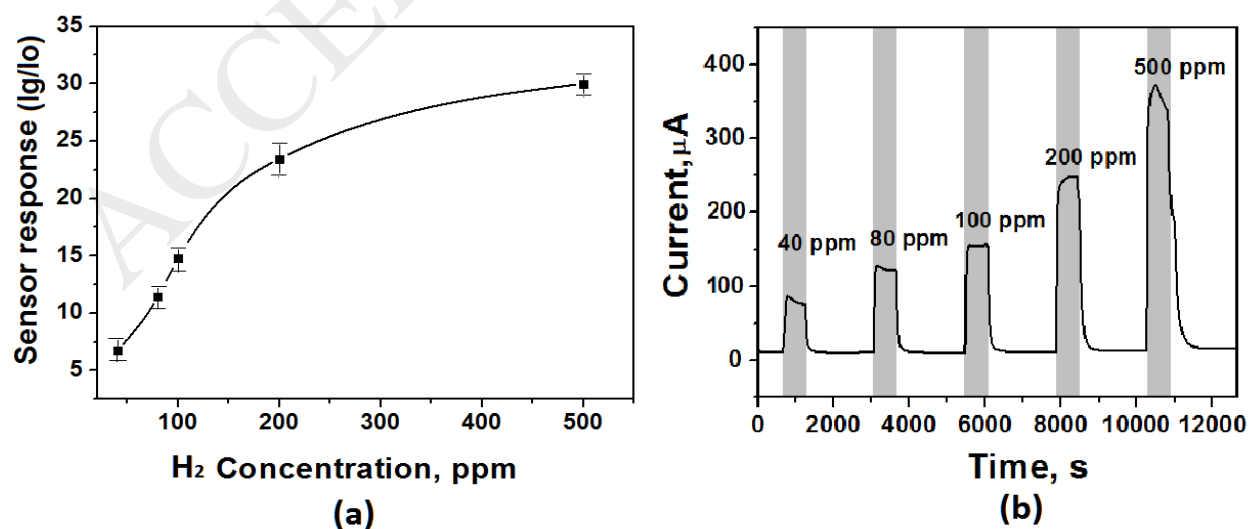


Figure 14 (a) Evolution of sensor response (and associated error bars) as a function of H₂ concentration.

(b) Current flowing through the gas sensitive film when sensor is exposed to pulses (gray lines, 10 min.) of increasing concentration of H₂. The baseline current is recovered by blowing the sensor with dry air (30 min.).

4. Conclusions

A new planar architecture has been proposed for heated gas sensors. The new approach uses one of the sensing electrodes simultaneously as heating element. In contrast with standard topologies using independent heater and electrodes, this approach results in the following benefits for printed metal-oxide sensors: reducing the consumption of expensive metallic inks, decreasing of the substrate area needed for the transducer in a planar configuration, and, in comparison to a stack configuration, it avoids the constraint of printing robust inter-dielectric layer. The operation of the new topology has been simulated (FEM) with Comsol Multiphysics and the developed model has been experimentally validated. To demonstrate the operation of the architecture for gas sensing, a set of electrodes have been inkjet-printed and coated by the in-situ growth via AA-CVD of an active layer consisting of nanoparticle decorated WO₃ nanowires. The resulting devices have been characterized as H₂ sensors and results were completely satisfactory, being comparable to those obtained on standard silicon micromachined transducers. The proposed planar architecture has been proven to work as an efficient strategy to simplify the manufacturing of metal oxide gas sensors on polymeric foil, but could be applied also to metal-oxide gas sensors made on the traditional ceramic and silicon substrates. We are now considering printing techniques with a higher resolution to reduce the footprint of the transducer and therefore reduced significantly its power consumption.

Acknowledgements

This work was supported in part by the COST TD 1105 Action “EuNetAir”, by MINECO and the European Funds for Regional Development via grant no. TEC2015-71663-R. E.L. is supported by the Catalan Institution for Research and Advanced Studies via the 2012 ICREA Academia Award.

REFERENCES

- [1] G. Korotcenkov, Handbook of Gas Sensor Materials Properties, Advantages and Shortcomings for Applications, Vol. 1: Conventional Approaches, p. 167-195, Springer, 2013.
- [2] Figaro Engineering Inc., Osaka, Japan, <http://www.figaro.co.jp/en/>, accessed June 2017.
- [3] C. Bittencourt, E. Llobet, P. Ivanov, X. Correig, X. Vilanova, J. Brezmes, J. Hubalek, K. Malysz, J.J. Pireaux, J. Calderer. “Influence of the doping method on the sensitivity of Pt-doped screen-printed SnO₂ sensors”; Sensors and Actuators B 97 67–73. 2004
- [4] Rieu, M., Camara, M., Tournier, G., Viricelle, J. Pijolat, C., de Rooij, N.F. & Briand, D. "Fully inkjet printed SnO₂ gas sensor on plastic substrate", Sensors and Actuators, B: Chemical, vol. 236, pp. 1091-1097. 2016.
- [5] E. Llobet, P. Ivanova, X. Vilanova, J. Brezmes, J. Hubalek, K. Malysz, I. Gràcia, C. Cané, X. Correig; “Screen-printed nanoparticle tin oxide films for high-yield sensor microsystems”; Sensors and Actuators B 96, 94–104, (2003).
- [6] A. Tomasi, M. Cocuzza, D. Perrone, C. Fabrizio Pirri, R. Mosca, M. Villani, N. Delmonte, A. Zappettini, D. Calestani, S.L. Matasso. “Modeling, fabrication and testing of a customizable

micromachined hotplate for sensor applications". Sensors, 17, 62; 2017.
doi:10.3390/s17010062

- [7] Sheng Yi, Shouquin Tian, Dawen Zeng, Keng Xu, Shuping Zhang, Changseng Xie, "An InO nanowire-like network fabricated on coplanar sensor surface by sacrificial CNTs for enhanced gas sensing performance", Sensors and Actuators B: Chemical, v 185, pp 345-353. 2013. doi: 10.1016/j.snb.2013.05.007
- [8] Alessio Giberti, Vincenzo Guidi, Donato Vincenzi. "A study of heat distribution and dissipation in a micromachined chemoresistive gas sensor". Sensors and Actuators B: Chemical, doi:10.1016/j.snb.2010.11.007
- [9] Alexia Bontempi, Laurent Thiery, Damien Teyssieux, Danick Briand, Pascal Vairac. "Quantitative thermal microscopy using thermoelectric probe in passive mode". Review of Scientific Instruments, American Institute of Physics, 2013, 84, pp.103703.
- [10] Astie, S., A. Gue, E. Scheid, and J. Guillemet, "Design of a low power SnO₂ gas sensor integrated on silicon oxynitride membrane". SENSORS AND ACTUATORS BCHEMICAL, pp. 84-88. 2000.
- [11] Rossi, C., E. Scheid, and D. Esteve, "Theoretical and experimental study of silicon micromachined microheater with dielectric stacked membranes". SENSORS AND ACTUATORS A-PHYSICAL, 1997.
- [12] Sabaté, N., Santander, J., Gràcia, I., Fonseca, L., Figueras, E., Cabruja, E., Cané, C.; "Characterization of thermal conductivity in thin film multilayered membranes". Thin solid Films, Elsevier, 2005
- [13] The engineering Toolbox, "Emissivity Coefficients of some common Materials", on line, http://www.engineeringtoolbox.com/emissivity-coefficients-d_447.html, [last download: Feb 13th, 2017].
- [14] Vallejos, S.; Umek, P.; Stoycheva, T.; Annanouch, F.; Llobet, E.; Correig, X.; de Marco, P.; Bittencourt, C.; Blackman, C., Single-step deposition of Au- and Pt-nanoparticle-functionalized tungsten oxide nanoneedles synthesized via aerosol-assisted CVD, and used for fabrication of selective gas microsensor arrays, *Adv. Func. Mat.* 2013, 23, 1313.
- [15] Vallejos, S.; Stoycheva, T.; Annanouch, F.E.; Llobet, E.; Umek, P.; Figueras, E.; Canè, C.; Gràcia, I.; Blackman, C., Microsensors based on Pt-nanoparticle functionalised tungsten oxide nanoneedles for monitoring hydrogen sulfide, *RSC Advances*, 2014, 4, 1489-1495.
- [16] S. Vallejos, I. Gràcia, O. Chmela, E. Figueras, J. Hubálek, C. Cané, Chemoresistive micromachined gas sensors based on functionalized metal oxide nanowires: Performance and reliability, Sensors and Actuators B: Chemical, Volume 235, 2016, Pages 525-534

Biography

Jose Luis Ramirez (Reus, 1970) received his Telecommunications engineering degree in 1994 from Universitat Politècnica de Catalunya in Barcelona, Spain. He obtained his PhD. In the field of analog microelectronic design, from UPC in 2003. He is currently associate professor at Universitat Rovira i Virgili (Tarragona, Spain). His main research topics are related to transducers for sensing microsystems, digital/analog microelectronics and microcontroller based designs.

Fatima Ezahra Annanouch was born in Morocco, 1986. She graduated in Physics from the Moulay Ismail University in Meknes, Morocco. She obtained her Ph.D. degree in the field of sensor microsystems from the Electronic Engineering Department, University Rovira i Virgili, Tarragona, Spain. She is currently holding a postdoc position at the Institut Matériaux Microélectronique Nanosciences de Provence/Aix-Marseille Université, France.

Eduard Llobet Eduard Llobet (Barcelona, 1967) is a full professor at the Universitat Rovira i Virgili. During 2010–2014 he was Director of the Research Centre on Engineering of Materials and micro/nano Systems. In 2012 he received the ICREA Academia Award. Prof. Llobet works in the growth and functionalization of inorganic and carbon nanomaterials and their applications in gas sensing, catalysis, or energy.

Danick Briand received his B.Eng. degree and M.A.Sc. degree in engineering physics from École Polytechnique in Montréal, Canada, in collaboration with the Institut National Polytechnique de Grenoble (INPG), France, in 1995 and 1997, respectively. He obtained his PhD degree in the field of micro-chemical sensing systems from the Institute of Microtechnology (IMT), University of Neuchâtel, Switzerland in 2001. He is currently at Microsystems for Space Technologies Laboratory, at EPFL IMT. He has been awarded the Euroensors Fellowship in 2010. He has been author or co-author on more than 200 papers published in scientific journals and conference proceedings. His research interests include polymeric MEMS, Power MEMS and energy harvesting, autonomous smart sensing systems, and printed and flexible microsystems technologies.